Electronic Supplementary Material (ESI) for Journal of Materials Chemistry A.

Electronic Supporting Information for First-principles Study for Discovery of Novel Synthesizable 2D High-Entropy Transition Metal Carbides (MXenes)

Hyun Woo Seong[a], Min Seok Lee[a], Ho Jin Ryu*[a]

[a] Department of Nuclear and Quantum Engineering, KAIST, Daejeon 34141, Republic of Korea.

*E-mail: hojinryu@kaist.ac.kr, Fax: +82-42-350-8912.

ESI Note 1. Thermodynamic stability of HE-MAX phases

One of the methods to predict thermodynamic stability is to determine whether the formation energy is negative. For a general k-$M_{n+1}AX_n$ phase (k = 4 or 5), the formation energy per atom, ΔE_f is obtained as

$$\Delta E_f\,(k\text{-}M_{n+1}AX_n) = E(k\text{-}M_{n+1}AX_n) - \left\{(n+1)\sum_{i=1}^{k} E_i^M/k + E^A + nE^X\right\}/(2n+2) \quad (1)$$

where $E(k\text{-}M_{n+1}AX_n)$ represents the total energy per atom of k-$M_{n+1}AX_n$ phase and E^j with $j \in \{M, A, X\}$ corresponds to the total energy per atom of their ground-state crystal structure.

However, although the HE-MAX phase might be energetically favorable compared to the constituent elements, it will not be synthesized if there are competing phases that are more energetically favorable than the HE-MAX phase. This means that several competing phases might exist in the given composition and the more energetically favorable competing phases are likely to be synthesized instead.[1] Therefore, in this study, we determined the thermodynamic stability of the HE-MAX phases using relative Gibbs free energy, which means the difference in Gibbs energy between the HE-MAX phase and its competing phases.[2,3] There are temperature contributions to Gibbs free energy, such as vibrational, electronic, magnetic, and configurational entropy. However, in the case of a high-entropy system, electronic and magnetic entropy are often negligible because their values are imperceptible compared to vibrational and configurational entropy.[4] Additionally, Thore et al.[3] investigated that the vibrational contribution tends to be canceled out between the MAX phases and the competing phases. Therefore, the relative Gibbs free energy per atom of k-$M_{n+1}AX_n$ phase at T K, ΔG_{Re}^T can be expressed as

$$\Delta G_{Re}^T(k\text{-}M_{n+1}AX_n) = \Delta H_{Re}(k\text{-}M_{n+1}AX_n) - T\Delta S_{Re}^{conf}\,(k\text{-}M_{n+1}AX_n) \quad (2)$$

where $\Delta H_{Re}(k\text{-}M_{n+1}AX_n)$ is the relative formation enthalpy per atom of k-$M_{n+1}AX_n$ phase at 0 K, ΔS_{Re}^{conf} is the relative configurational entropy per atom of k-$M_{n+1}AX_n$ phase, and T is the temperature. If the $\Delta G_{Re}^T(k\text{-}M_{n+1}AX_n)$ is negative, k-$M_{n+1}AX_n$ phase is considered as thermodynamically stable at T. The more negative ΔG_{Re}^T value means, the higher the probability of successful experimental synthesis.

The enthalpy of formation at T K can be obtained by using Equation S(3). However, it is computationally expensive to obtain the molar heat capacity (C_V) of a novel material. For that reason, in many previous papers, the enthalpy of formation at 0 K was used instead of the enthalpy of formation at T K to explore new materials.[5–7] Because the enthalpy of formation is calculated as the difference in enthalpy between constituent materials, the temperature-dependent error of the enthalpy of formation is negligible; the error is within 0.03 eV/atom at 298 K.[8,9] Therefore, only the relative formation enthalpies at 0 K were considered in this study.

$$\Delta H^T = \Delta H^{0\,K} + \int_0^T \Delta C_V\, dT \quad (3)$$

The relative formation enthalpy per atom of k-$M_{n+1}AX_n$ phase at 0 K, ΔH_{Re} is often called as energy above the convex hull and is calculated according to

$$\Delta H_{Re}(k\text{-}M_{n+1}AX_n) = E(k\text{-}M_{n+1}AX_n) - E_{cp}\,(k\text{-}M_{n+1}AX_n) \quad (4)$$

where E_{cp} $(k\text{-}M_{n+1}AX_n)$ represents the total energy per atom of the linear combinations of the most competing phases for a given $k\text{-}M_{n+1}AX_n$, respectively. The competing phase candidates for HE-MAX phases consist of single elements, binary compounds, and ternary compounds available in the open quantum materials database (OQMD).[10,11] Their total energy per atom was also acquired from the OQMD. We randomly selected 10 competing phase candidates (Ti_3SiC_2, VCr, Cr_2Al, $ZrAl_2$, $NbTa_2$, Mo_3Al, Mo_2C, HfTaSi, Ta_2C, Si) and calculated total energy per atom to confirm the magnitude of the energy error between OQMD and this work. The average of the absolute error is 0.02 eV/atom. The set of most competing phases was searched by using a linear algebra and linear algorithm.[2]

The configurational entropy of the most competing phases is zero because the competing phase candidates included in this study are compositionally ordered. Consequently, the relative configurational entropy of $k\text{-M}_{n+1}\text{AX}_n$ phase is identical to the configurational entropy of $k\text{-M}_{n+1}\text{AX}_n$ phase and it can be obtained from the sub-lattice model.[4,12] The configurational entropy per atom of sub-lattice structure, S_{SL}^{conf} is defined as

$$\text{S}_{SL}^{conf} = -k_B \left(\sum_x \sum_{i=1}^{N^x} a^x f_i^x \ln(f_i^x) \right) / \sum_x a^x \tag{5}$$

where k_B is the Boltzmann constant. a^x means the number of sites on the x sub-lattice and $\sum_x a^x$ means the total number of atoms per formula unit. N^x means the total number of element species in the x sub-lattice. f_i^x means the mole fraction of component i, which is randomly distributed in the x sub-lattice.

ESI Note 2. Exfoliation possibility of HE-MAX phases to HE-MXenes

Hydrofluoric (HF) acid is widely employed for the selective etching of A-elements in MAX phases. The chemical etching reaction of the MAX phases can be approximated by the following equations[13]:

$$\mathrm{M}_{n+1}\mathrm{AlX}_n + 3\mathrm{HF} \rightarrow \mathrm{M}_{n+1}\mathrm{X}_n + \mathrm{AlF}_3 + 1.5\mathrm{H}_2 \quad (6)$$

$$\mathrm{M}_{n+1}\mathrm{SiX}_n + 4\mathrm{HF} \rightarrow \mathrm{M}_{n+1}\mathrm{X}_n + \mathrm{SiF}_4 + 2\mathrm{H}_2 \quad (7)$$

$$\mathrm{M}_{n+1}\mathrm{X}_n + 2\mathrm{HF} \rightarrow \mathrm{M}_{n+1}\mathrm{X}_n\mathrm{F}_2 + \mathrm{H}_2 \quad (8)$$

$$\mathrm{M}_{n+1}\mathrm{X}_n + 2\mathrm{H}_2\mathrm{O} \rightarrow \mathrm{M}_{n+1}\mathrm{X}_n\mathrm{O}_2 + 2\mathrm{H}_2 \quad (9)$$

$$\mathrm{M}_{n+1}\mathrm{X}_n + 2\mathrm{H}_2\mathrm{O} \rightarrow \mathrm{M}_{n+1}\mathrm{X}_n(\mathrm{OH})_2 + \mathrm{H}_2 \quad (10)$$

However, the chemical exfoliation process is difficult to simulate in detail due to its complicated environments such as the temperature, etching time, and concentration of the acid. Furthermore, the compositions and ratio of surface terminators of MXenes vary depending on the synthesis procedure. Due to these problems, previous studies evaluated the exfoliation possibility in consideration of the mechanical exfoliation process.[14–18] In this study, we analyzed the exfoliation possibility of HE-MAX phases to HE-MXenes using two perspectives: mechanical exfoliation and simplified chemical exfoliation.

The mechanical exfoliation energy, called as static exfoliation energy, $\mathrm{E}_{\mathrm{ex}}^{m\ e}$ is calculated from the following equation.

$$\mathrm{E}_{\mathrm{ex}}^{m\ e}(k\text{-}\mathrm{M}_{n+1}\mathrm{AX}_n) = \{(2n+1)E(k\text{-}\mathrm{M}_{n+1}\mathrm{X}_n) + E^A - (2n+2)E(k\text{-}\mathrm{M}_{n+1}\mathrm{AX}_n)\}/2S \quad (11)$$

Here, $E(k\text{-}\mathrm{M}_{n+1}\mathrm{X}_n)$ and $E(k\text{-}\mathrm{M}_{n+1}\mathrm{AX}_n)$ are the total energy per atom of $k\text{-}\mathrm{M}_{n+1}\mathrm{X}_n$ and $k\text{-}\mathrm{M}_{n+1}\mathrm{AX}_n$ phases, respectively, E^A is the total energy per atom of the ground-state crystal structure of A-element, and S means the surface area of the unit cell of the $k\text{-}\mathrm{M}_{n+1}\mathrm{AX}_n$ phase. By using Equation (5) and (6), we defined the simplified chemical exfoliation energy per atom of $k\text{-}\mathrm{M}_{n+1}\mathrm{AX}_n$ phase, $\mathrm{E}_{\mathrm{ex}}^{ch}$ as

$$\mathrm{E}_{\mathrm{ex}}^{ch}(k\text{-}\mathrm{M}_{n+1}\mathrm{AlX}_n) = \{(2n+1)E(k\text{-}\mathrm{M}_{n+1}\mathrm{X}_n) + 4E(\mathrm{AF}_3) + 3E(\mathrm{H}_2) - (2n+2)E(k\text{-}\mathrm{M}_{n+1}\mathrm{AlX}_n) - 6E(\mathrm{HF})\}/(2n+8) \quad (12)$$

$$\mathrm{E}_{\mathrm{ex}}^{ch}(k\text{-}\mathrm{M}_{n+1}\mathrm{SiX}_n) = \{(2n+1)E(k\text{-}\mathrm{M}_{n+1}\mathrm{X}_n) + 5E(\mathrm{SiF}_4) + 4E(\mathrm{H}_2) - (2n+2)E(k\text{-}\mathrm{M}_{n+1}\mathrm{SiX}_n) - 8E(\mathrm{HF})\}/(2n+10) \quad (13)$$

where $E(phase)$ is the total energy per atom of each ground-state phase at 0 K. In the case of both $\mathrm{E}_{\mathrm{ex}}^{m\ e}$ and $\mathrm{E}_{\mathrm{ex}}^{ch}$, the lower the exfoliation energy, the higher the exfoliation possibility.

ESI Note 3. Convergence test of the cut-off energy and *k*-points

The values of cut-off energy and *k*-points density are motivated by converging the formation energy of MAX phases. We select the Nb_2AlC, Ti_3SiC_2, and Ta_4AlC_3 phases as representatives of the MAX phases. As shown Fig. S1, the values of cut-off energy above 450 eV and *k*-points spacing density below 0.3 Å^{-1} ensure formation energy convergence to within 1 meV/atom. In this study, because of compatibility with OQMD, the plane-wave basis set with a 520 eV cut-off energy was employed and the *k*-points spacing density was set to within 0.15 Å^{-1}.

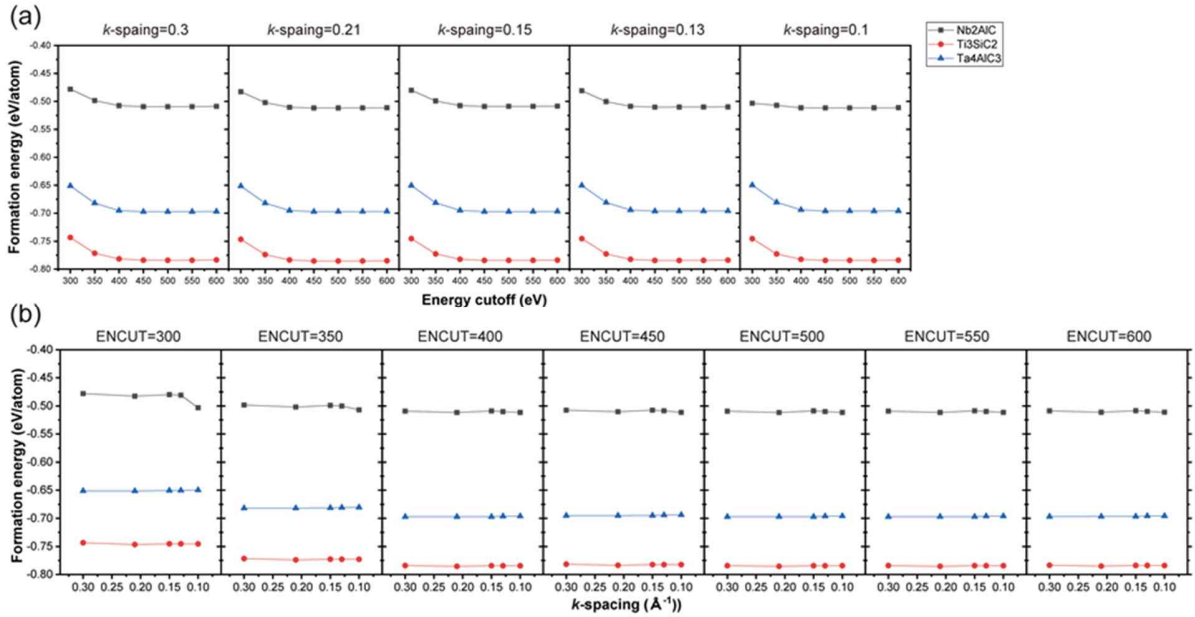

Fig. S1 Convergence test of the formation energy for Nb2AlC, Ti3SiC2, and Ta4AlC3 phases as a function of (a) the cut-off energy for various k-spacings and (b) the k-spacing for various cut-off energies.

ESI Note 4. Crystal structrures of SQS supercells and permutation tests

Since SQS supercells are approximations of random structures**,** there is an error in representing random solid solution configurations. To qualify for our calculated SQS supercells, we performed permutation tests which are calculating the standard deviation of the energies for all permutations obtained by swapping between elemental species.[19,20] For a high-entropy material with *n* equiatomic elements, there are *n*! possible permutations. For instance, In this study, the standard deviations are less than 1.5 meV/atom. In other words, considering the 95% confidence interval, the margin of error for the SQS structures is less than 3meV/atom.

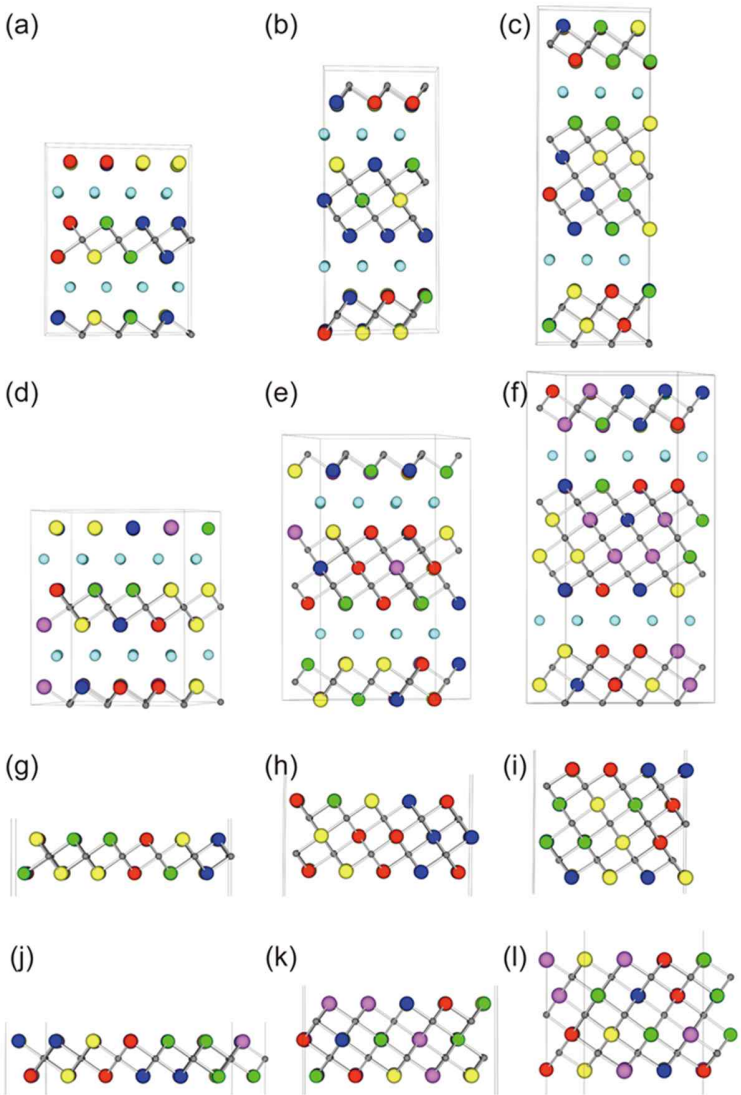

Fig. S2 Crystal structures of the SQS supercells for (a) 4-M_2AX (128 atoms), (b) 4-M_3AX_2 (144 atoms), (c) 4-M_4AX_3 (144 atoms), (d) 5-M_2AX (120 atoms), (e) 5-M_3AX_2 (120 atoms), (f) 5-M_4AX_3 (160 atoms), (g) 4-M_2X (108 atoms), (h) 4-M_3X_2 (100 atoms), (i) 4-M_4X_3 (112 atoms), (j) 5-M_2X (105 atoms), (k) 5-M_3X_2 (120 atoms), and (l) 5-M_4X_3 (125 atoms

ESI Note 5. List of synthesized single M MAX phases, predicted HE-MAX phases, corresponding competing phases, and predicted HE-MXenes

Table S1 List of experimentally synthesized ternary transition metal carbide (MAX) phases with Al and Si.[18,21]

Type (Total number)	Predicted HE-MAX phases
M_2AX	Ti_2AlC, V_2AlC, Cr_2AlC, Zr_2AlC, Nb_2AlC, Ta_2AlC
M_3AX_2	Ti_3AlC_2, V_3AlC_2, Zr_3AlC_2, Ta_3AlC_2, Ti_3SiC_2
M_4AX_3	Ti_4AlC_3, V_4AlC_3, Nb_4AlC_3, Ta_4AlC_3, Ti_4SiC_3

Table S2 List of predicted HE-MAX phases using relative Gibbs free energy. Synthesized HE-MAX phases reported to date are highlighted in bold.

Type (Total number)	Predicted HE-MAX phases
4-$M_{n+1}AlC_n$ (81)	$(TiVCrNb)_2AlC$, $(TiVCrMo)_2AlC$, $(TiVCrTa)_2AlC$, $(TiVZrNb)_2AlC$, $(TiVZrMo)_2AlC$, $(TiVZrHf)_2AlC$, $(TiVZrTa)_2AlC$, $(TiVNbMo)_2AlC$, $(TiVNbHf)_2AlC$, $(TiVNbTa)_2AlC$, $(TiVMoTa)_2AlC$, $(TiVHfTa)_2AlC$, $(TiCrNbMo)_2AlC$, $(TiCrNbTa)_2AlC$, $(TiCrMoTa)_2AlC$, $(TiZrNbMo)_2AlC$, $(TiZrNbHf)_2AlC$, **$(TiZrNbTa)_2AlC$**, $(TiZrMoTa)_2AlC$, $(TiZrHfTa)_2AlC$, $(TiNbMoHf)_2AlC$, $(TiNbMoTa)_2AlC$, $(TiNbHfTa)_2AlC$, $(TiMoHfTa)_2AlC$, $(VCrNbMo)_2AlC$, $(VZrNbMo)_2AlC$, $(VZrNbHf)_2AlC$, $(VZrNbTa)_2AlC$, $(VNbMoTa)_2AlC$, $(VNbHfTa)_2AlC$, $(ZrNbMoTa)_2AlC$, $(ZrNbHfTa)_2AlC$, $(TiVCrNb)_3AlC_2$, $(TiVCrMo)_3AlC_2$, $(TiVCrTa)_3AlC_2$, $(TiVZrNb)_3AlC_2$, $(TiVZrTa)_3AlC_2$, $(TiVNbMo)_3AlC_2$, $(TiVNbHf)_3AlC_2$, $(TiVNbTa)_3AlC_2$, $(TiVMoTa)_3AlC_2$, $(TiVHfTa)_3AlC_2$, $(TiZrNbMo)_3AlC_2$, $(TiZrNbHf)_3AlC_2$, $(TiZrNbTa)_3AlC_2$, $(TiZrMoTa)_3AlC_2$, $(TiZrHfTa)_3AlC_2$, $(TiNbMoHf)_3AlC_2$, $(TiNbMoTa)_3AlC_2$, $(TiNbHfTa)_3AlC_2$, $(TiMoHfTa)_3AlC_2$, $(VZrNbTa)_3AlC_2$, $(VNbHfTa)_3AlC_2$, $(ZrNbMoTa)_3AlC_2$, $(ZrNbHfTa)_3AlC_2$, **$(TiVCrMo)_4AlC_3$**, $(TiVCrTa)_4AlC_3$, $(TiVZrNb)_4AlC_3$, $(TiVZrTa)_4AlC_3$, **$(TiVNbMo)_4AlC_3$**, $(TiVNbTa)_4AlC_3$, $(TiVMoTa)_4AlC_3$, $(TiVHfTa)_4AlC_3$, $(TiCrNbTa)_4AlC_3$, $(TiZrNbMo)_4AlC_3$, $(TiZrNbHf)_4AlC_3$, $(TiZrNbTa)_4AlC_3$, $(TiZrMoTa)_4AlC_3$, $(TiZrHfTa)_4AlC_3$, $(TiNbMoHf)_4AlC_3$, $(TiNbMoTa)_4AlC_3$, $(TiNbHfTa)_4AlC_3$, $(TiMoHfTa)_4AlC_3$, $(VZrNbTa)_4AlC_3$, $(VNbMoTa)_4AlC_3$, $(VNbHfTa)_4AlC_3$, $(ZrNbMoHf)_4AlC_3$, $(ZrNbMoTa)_4AlC_3$, $(ZrNbHfTa)_4AlC_3$, $(ZrMoHfTa)_4AlC_3$, $(NbMoHfTa)_4AlC_3$
4-$M_{n+1}SiC_n$ (18)	$(TiVNbTa)_2SiC$, $(TiVZrTa)_3SiC_2$, $(TiVNbTa)_3SiC_2$, $(TiZrNbHf)_3SiC_2$, $(TiZrNbTa)_3SiC_2$, $(TiZrHfTa)_3SiC_2$, $(TiNbHfTa)_3SiC_2$, $(ZrNbHfTa)_3SiC_2$, $(TiVZrNb)_4SiC_3$, $(TiVZrTa)_4SiC_3$, $(TiVNbTa)_4SiC_3$, $(TiVHfTa)_4SiC_3$, $(TiZrNbMo)_4SiC_3$, $(TiZrNbHf)_4SiC_3$, $(TiZrNbTa)_4SiC_3$, $(TiZrHfTa)_4SiC_3$, $(TiNbHfTa)_4SiC_3$, $(ZrNbHfTa)_4SiC_3$
5-$M_{n+1}AlC_n$ (65)	$(TiVCrNbMo)_2AlC$, $(TiVCrNbTa)_2AlC$, $(TiVCrMoTa)_2AlC$, $(TiVZrNbMo)_2AlC$, $(TiVZrNbHf)_2AlC$, **$(TiVZrNbTa)_2AlC$**, $(TiVZrMoTa)_2AlC$, $(TiVZrHfTa)_2AlC$, $(TiVNbMoHf)_2AlC$, $(TiVNbMoTa)_2AlC$, $(TiVNbHfTa)_2AlC$, $(TiVMoHfTa)_2AlC$, $(TiCrNbMoTa)_2AlC$, $(TiZrNbMoHf)_2AlC$, $(TiZrNbMoTa)_2AlC$, **$(TiZrNbHfTa)_2AlC$**, $(TiZrMoHfTa)_2AlC$, $(TiNbMoHfTa)_2AlC$, $(VCrNbMoTa)_2AlC$, $(VZrNbMoTa)_2AlC$, $(VZrNbHfTa)_2AlC$, $(VNbMoHfTa)_2AlC$, $(ZrNbMoHfTa)_2AlC$, $(TiVCrNbMo)_3AlC_2$, $(TiVCrNbTa)_3AlC_2$, $(TiVCrMoTa)_3AlC_2$, $(TiVZrNbMo)_3AlC_2$, $(TiVZrNbHf)_3AlC_2$, $(TiVZrNbTa)_3AlC_2$, $(TiVZrMoTa)_3AlC_2$, $(TiVZrHfTa)_3AlC_2$, $(TiVNbMoHf)_3AlC_2$, $(TiVNbMoTa)_3AlC_2$, $(TiVNbHfTa)_3AlC_2$, $(TiVMoHfTa)_3AlC_2$, $(TiCrNbMoTa)_3AlC_2$, $(TiZrNbMoHf)_3AlC_2$, $(TiZrNbMoTa)_3AlC_2$, $(TiZrNbHfTa)_3AlC_2$, $(TiZrMoHfTa)_3AlC_2$, $(TiNbMoHfTa)_3AlC_2$, $(VZrNbMoTa)_3AlC_2$, $(VZrNbHfTa)_3AlC_2$, $(ZrNbMoHfTa)_3AlC_2$, $(TiVCrNbMo)_4AlC_3$, **$(TiVCrNbTa)_4AlC_3$**, $(TiVCrMoTa)_4AlC_3$, $(TiVZrNbMo)_4AlC_3$, $(TiVZrNbHf)_4AlC_3$, $(TiVZrNbTa)_4AlC_3$, $(TiVZrMoTa)_4AlC_3$, $(TiVZrHfTa)_4AlC_3$, $(TiVNbMoHf)_4AlC_3$, $(TiVNbMoTa)_4AlC_3$, $(TiVNbHfTa)_4AlC_3$, $(TiVMoHfTa)_4AlC_3$, $(TiCrNbMoTa)_4AlC_3$, $(TiZrNbMoHf)_4AlC_3$, $(TiZrNbMoTa)_4AlC_3$, $(TiZrNbHfTa)_4AlC_3$, $(TiZrMoHfTa)_4AlC_3$, $(TiNbMoHfTa)_4AlC_3$, $(VZrNbMoTa)_4AlC_3$, $(VZrNbHfTa)_4AlC_3$, $(ZrNbMoHfTa)_4AlC_3$
5-$M_{n+1}SiC_n$ (11)	$(TiVZrNbTa)_3SiC_2$, $(TiVZrHfTa)_3SiC_2$, $(TiVNbHfTa)_3SiC_2$, $(TiZrNbHfTa)_3SiC_2$, $(TiVZrNbHf)_4SiC_3$, $(TiVZrNbTa)_4SiC_3$, $(TiVZrHfTa)_4SiC_3$, $(TiVNbHfTa)_4SiC_3$, $(TiZrNbMoTa)_4SiC_3$, $(TiZrNbHfTa)_4SiC_3$, $(VZrNbHfTa)_4SiC_3$

Table S3 List of competing phases corresponding to predicted HE-MAX phases.

Predicted HE-MAX	Competing phases	Predicted HE-MAX	Competing phases
$(TiVCrNb)_2AlC$	V_2AlC,$NbAl_3$,Nb_3AlC_2,Cr_2Al,TiC *	$(TiVCrMo)_2AlC$	V_6C_5, Mo_3Al, Mo_3Al_8, $Cr_{21}Mo_2C_6$, Cr_2Al, TiC
$(TiVCrTa)_2AlC$	V_2AlC, Ti_3AlC_2, $CrAl_3$, Ta_3AlC_2, Cr_2Al, TiC	$(TiVZrNb)_2AlC$	V_2AlC, Nb_2AlC, Ti_3AlC_2, Zr_6C_5, $ZrAl_2$, Nb_2Al
$(TiVZrMo)_2AlC$	V_2AlC, Ti_3AlC_2, ZrC, $ZrAl_2$, Mo_3Al, Mo_3Al_8	$(TiVZrHf)_2AlC$	V_2AlC, Zr_6C_5, Hf_6C_5, $ZrAl_2$, Zr_4Al_3, Ti_2AlC
$(TiVZrTa)_2AlC$	V_2AlC, Ti_3AlC_2, Zr_6C_5, $ZrAl_2$, V, Ta_2C	$(TiVNbMo)_2AlC$	V_2AlC, Mo_3Al_8, Nb_3AlC_2, Ti_6C_5, Mo_3Al
$(TiVNbHf)_2AlC$	V_2AlC, HfC, $NbAl_3$, Nb_2Al, Ti_2AlC	$(TiVNbTa)_2AlC$	V_2AlC, Nb_2AlC, Ti_3AlC_2, $NbAl_3$, Ta_2C, Nb_3Al_2C
$(TiVMoTa)_2AlC$	V_2AlC, Ti_3AlC_2, Mo_3Al_8, Mo_3Al, Ta_6C_5	$(TiVHfTa)_2AlC$	V_2AlC, HfC, $TiAl_2$, Hf_3AlC_2, Ta_2C, Ti_2AlC
$(TiCrNbMo)_2AlC$	Mo_3Al_8, Nb_6C_5, $Cr_{23}C_6$, Mo_3Al, Cr_2Al, TiC	$(TiCrNbTa)_2AlC$	Nb_2AlC, $NbAl_3$, Nb_3AlC_2, Ti_6C_5, Cr_2Al, Ta_6C_5
$(TiCrMoTa)_2AlC$	Mo_3Al_8, Mo_3Al, $Cr_2Mo_2C_6$, Cr_2Al, TiC, Ta_6C_5	$(TiZrNbMo)_2AlC$	Nb_2AlC, Ti_3AlC_2, ZrC, $NbAl_3$, Mo_3Al
$(TiZrNbHf)_2AlC$	Ti_3AlC_2, Zr_6C_5, $ZrAl_2$, HfC, Nb_2Al, Ti_2AlC	$(TiZrNbTa)_2AlC$	Nb_2AlC, Ti_3AlC_2, Zr_6C_5, $ZrAl_2$, Ta_2C, Nb_3Al_2C
$(TiZrMoTa)_2AlC$	ZrC, Ti_3AlC_2, $ZrAl_2$, Mo_3Al_8, Ta_2C, Mo_3Al	$(TiZrHfTa)_2AlC$	Ti_3AlC_2, $ZrAl_2$, Zr_2Al_3, Ta_2C, Hf_6C_5
$(TiNbMoHf)_2AlC$	Nb_2AlC, Ti_3AlC_2, HfC, $NbAl_3$, Mo_3Al	$(TiNbMoTa)_2AlC$	$NbAl_3$, Nb_3AlC_2, Ti_6C_5, Mo_3Al, Ta_6C_5
$(TiNbHfTa)_2AlC$	HfC, $NbAl_3$, Nb_2Al, Ta_2C, Ti_2AlC	$(TiMoHfTa)_2AlC$	HfC, Mo_3Al_8, Ta_2C, Mo_3Al, Ti_2AlC
$(VCrNbMo)_2AlC$	V_6C_5, Cr_7C_3, Mo_3Al_8, Nb_6C_5, $Cr_{23}C_6$, Mo_3Al	$(VZrNbMo)_2AlC$	V_2AlC, $NbAl_3$, Mo_3Al_8, Nb_3AlC_2, Mo_3Al, ZrC
$(VZrNbHf)_2AlC$	V_2AlC, Zr_6C_5, $ZrAl_2$, HfC, $NbAl_3$, Nb_2Al	$(VZrNbTa)_2AlC$	V_2AlC, ZrC, Nb_2AlC, $ZrAl_2$, Ta_2C
$(VNbMoTa)_2AlC$	V_2AlC, Mo_3Al_8, Nb_3AlC_2, Mo_3Al, Ta_6C_5	$(VNbHfTa)_2AlC$	V_2AlC, HfC, $NbAl_3$, Nb_2Al, Ta_2C
$(ZrNbMoTa)_2AlC$	Nb_2AlC, ZrC, $NbAl_3$, Ta_2C, Mo_3Al, Ta_6C_5	$(ZrNbHfTa)_2AlC$	Zr_6C_5, $ZrAl_2$, HfC, Nb_2Al, Ta_2C, Nb_3Al_2C
$(TiVCrNb)_3AlC_2$	V_6C_5, Cr, Cr_7C_3, $NbAl_3$, Nb_6C_5, TiC	$(TiVCrMo)_3AlC_2$	V_6C_5, Mo_3Al_8, Cr_3C_2, $Ti_2Mo_2C_3$, $Cr_{21}Mo_2C_6$, TiC
$(TiVCrTa)_3AlC_2$	V_3AlC_2, $CrAl_3$, TaC, Cr_2Al, TiC	$(TiVZrNb)_3AlC_2$	V_2AlC, Nb_2AlC, Ti_3AlC_2, ZrC
$(TiVZrTa)_3AlC_2$	V_2AlC, ZrC, Ti_3AlC_2, Zr_6C_5, $ZrAl_2$, Ta_3AlC_2	$(TiVNbMo)_3AlC_2$	V_6C_5, Mo_3Al_8, Nb_6C_5, Mo_3Al, TiC
$(TiVNbHf)_3AlC_2$	V_2AlC, Nb_2AlC, Ti_3AlC_2, HfC	$(TiVNbTa)_3AlC_2$	V_2AlC, Nb_2AlC, $NbAl_3$, Nb_3AlC_2, Ti_6C_5, Ta_6C_5
$(TiVMoTa)_3AlC_2$	V_6C_5, Mo_3Al_8, Mo_3Al, TiC, Ta_6C_5	$(TiVHfTa)_3AlC_2$	V_2AlC, Ta_2AlC, Ti_3AlC_2, HfC
$(TiZrNbMo)_3AlC_2$	ZrC, Mo_3Al_8, Nb_3AlC_2, Mo_3Al, TiC	$(TiZrNbHf)_3AlC_2$	Nb_2AlC, Ti_3AlC_2, Zr_6C_5, $ZrAl_2$, HfC, Nb_2Al
$(TiZrNbTa)_3AlC_2$	ZrC, Nb_2AlC, $NbAl_3$, Ta_2C, Ti_6C_5	$(TiZrMoTa)_3AlC_2$	ZrC, Mo_3Al_8, Ti_6C_5, Mo_3Al, Ta_6C_5
$(TiZrHfTa)_3AlC_2$	ZrC, Ti_3AlC_2, $ZrAl_2$, HfC, Ta_2C	$(TiNbMoHf)_3AlC_2$	HfC, Mo_3Al_8, Nb_3AlC_2, Mo_3Al, TiC
$(TiNbMoTa)_3AlC_2$	Mo_3Al_8, Nb_6C_5, Mo_3Al, TiC, Ta_6C_5	$(TiNbHfTa)_3AlC_2$	Nb_2AlC, HfC, $NbAl_3$, Ta_2C, Ti_6C_5
$(TiMoHfTa)_3AlC_2$	HfC, Mo_3Al_8, Ti_6C_5, Mo_3Al, Ta_6C_5	$(VZrNbTa)_3AlC_2$	V_2AlC, ZrC, $NbAl_3$, Nb_3AlC_2, Ta_2C, Ta_6C_5
$(VNbHfTa)_3AlC_2$	V_2AlC, Nb_2AlC, HfC, Ta_3AlC_2	$(ZrNbMoTa)_3AlC_2$	ZrC, Zr_6C_5, Nb_6C_5, Mo_3Al, Ta_6C_5
$(ZrNbHfTa)_3AlC_2$	Nb_2AlC, Zr_6C_5, HfC, $NbAl_3$, Ta_2C	$(TiVCrMo)_4AlC_3$	V_6C_5, C, Mo_3Al_8, Cr_3C_2, $Ti_2Mo_2C_3$, TiC
$(TiVCrTa)_4AlC_3$	V_6C_5, V_3AlC_2, Al_4C_3, TaC, Cr_2Al, TiC	$(TiVZrNb)_4AlC_3$	V_2AlC, Nb_2AlC, ZrC, $NbAl_3$, Nb_6C_5, Ti_6C_5
$(TiVZrTa)_4AlC_3$	V_2AlC, ZrC, Ti_3AlC_2, $ZrAl_3$, TiC, Ta_6C_5	$(TiVNbMo)_4AlC_3$	V_6C_5, Mo_3Al_8, Nb_6C_5, $Ti_2Mo_2C_3$, TiC, C
$(TiVNbTa)_4AlC_3$	V_2AlC, $NbAl_3$, Nb_6C_5, Nb_3AlC_2, TiC, Ta_6C_5	$(TiVMoTa)_4AlC_3$	V_6C_5, Mo_3Al_8, TaC, Mo_3Al, $Ti_2Mo_2C_3$, TiC
$(TiVHfTa)_4AlC_3$	V_2AlC, Ti_3AlC_2, HfC, Ta_3AlC_2, TiC	$(TiCrNbTa)_4AlC_3$	$NbAl_3$, TaC, Nb_6C_5, Cr_3C_2, Cr_7C_3, TiC
$(TiZrNbMo)_4AlC_3$	ZrC, Mo_3Al_8, Nb_6C_5, Mo_3Al, TiC, MoC	$(TiZrNbHf)_4AlC_3$	Nb_2AlC, Ti_3AlC_2, Zr_6C_5, ZrC, HfC, $NbAl_3$
$(TiZrNbTa)_4AlC_3$	ZrC, Nb_2AlC, Ti_3AlC_2, $NbAl_3$, Ti_6C_5, Ta_6C_5	$(TiZrMoTa)_4AlC_3$	ZrC, Mo_3Al_8, TaC, Mo_3Al, TiC
$(TiZrHfTa)_4AlC_3$	Ta_2AlC, ZrC, Ti_3AlC_2, $ZrAl_3$, HfC, Ta_2C	$(TiNbMoHf)_4AlC_3$	HfC, Mo_3Al_8, Nb_6C_5, Mo_3Al, TiC, MoC
$(TiNbMoTa)_4AlC_3$	Mo_3Al_8, TaC, Nb_6C_5, Mo_3Al, $Ti_2Mo_2C_3$, TiC	$(TiNbHfTa)_4AlC_3$	Nb_2AlC, HfC, $NbAl_3$, Ti_6C_5, Ta_3AlC_2, Ta_6C_5
$(TiMoHfTa)_4AlC_3$	HfC, Mo_3Al_8, TaC, Mo_3Al, TiC	$(VZrNbTa)_4AlC_3$	V_2AlC, ZrC, $NbAl_3$, Nb_6C_5, Nb_3AlC_2, Ta_6C_5
$(VNbMoTa)_4AlC_3$	V_6C_5, $MoAl_3$, TaC, Nb_6C_5, Mo_2C	$(VNbHfTa)_4AlC_3$	V_2AlC, Nb_2AlC, HfC, $NbAl_3$, Nb_6C_5, Ta_6C_5
$(ZrNbMoHf)_4AlC_3$	HfC, Mo_3Al_8, Nb_6C_5, Mo_3Al, ZrC, MoC	$(ZrNbMoTa)_4AlC_3$	ZrC, Mo_3Al_8, TaC, Nb_6C_5, Mo_2C, Mo_3Al
$(ZrNbHfTa)_4AlC_3$	ZrC, HfC, $NbAl_3$, Nb_3AlC_2, Ta_2C	$(ZrMoHfTa)_4AlC_3$	ZrC, HfC, Mo_3Al_8, TaC, Mo_3Al
$(NbMoHfTa)_4AlC_3$	HfC, Mo_3Al_8, TaC, Nb_6C_5, Mo_2C, Mo_3Al	$(TiVNbTa)_2SiC$	$NbSi_2$, Nb_5Si_3C, V_5Si_3C, Ti_3SiC_2, TiC, Ta_6C_5
$(TiVZrTa)_3SiC_2$	ZrSi, V_6C_5, SiC, V_5Si_3C, TiC, Ta_6C_5	$(TiVNbTa)_3SiC_2$	$NbSi_2$, Nb_5Si_3C, V_6C_5, Ti_3SiC_2, TiC, Ta_6C_5
$(TiZrNbHf)_3SiC_2$	ZrSi, $NbSi_2$, Nb_5Si_3C, HfC, TiC, ZrC	$(TiZrNbTa)_3SiC_2$	ZrSi, $NbSi_2$, ZrC, Nb_5Si_3C, TiC, Ta_6C_5
$(TiZrHfTa)_3SiC_2$	ZrSi, SiC, TiC, HfC, Ti_3SiC_2, Ta_6C_5	$(TiNbHfTa)_3SiC_2$	$NbSi_2$, Ta_6C_5, Nb_5Si_3C, HfC, TaC, Ti_3SiC_2
$(ZrNbHfTa)_3SiC_2$	ZrSi, $NbSi_2$, ZrC, Nb_5Si_3C, HfC, TaC	$(TiVZrNb)_4SiC_3$	$NbSi_2$, V_6C_5, SiC, Nb_5Si_3C, TiC, ZrC
$(TiVZrTa)_4SiC_3$	ZrSi, V_6C_5, SiC, ZrC, TaC, TiC	$(TiVNbTa)_4SiC_3$	$NbSi_2$, Nb_5Si_3C, TaC, V_6C_5, Nb_6C_5, TiC
$(TiVHfTa)_4SiC_3$	V_6C_5, VSi_2, HfC, V_5Si_3C, TiC, Ta_6C_5	$(TiZrNbMo)_4SiC_3$	$Zr_2Mo_2C_3$, $MoSi_2$, Mo_5Si_3, Nb_6C_5, TiC, ZrC
$(TiZrNbHf)_4SiC_3$	ZrSi, $NbSi_2$, Nb_5Si_3C, HfC, TiC, ZrC	$(TiZrNbTa)_4SiC_3$	$NbSi_2$, ZrC, Nb_5Si_3C, TaC, TiC, Ta_6C_5
$(TiZrHfTa)_4SiC_3$	ZrSi, TiC, HfC, TaC	$(TiNbHfTa)_4SiC_3$	$NbSi_2$, Ta_6C_5, Nb_5Si_3C, HfC, TaC, TiC
$(ZrNbHfTa)_4SiC_3$	ZrSi, $NbSi_2$, ZrC, Nb_5Si_3C, HfC, TaC	$(TiVCrNbMo)_2AlC$	Cr_2Al, Mo_3Al, Mo_3Al_8, Nb_6C_5, TiC, V_2AlC, V_6C_5
$(TiVCrNbTa)_2AlC$	Cr_2Al, $NbAl_3$, Nb_3AlC_2, Ta_2C, Ta_6C_5, Ti_6C_5, V_2AlC	$(TiVCrMoTa)_2AlC$	Cr_2Al, Cr_7C_3, Mo_3Al, Mo_3Al_8, Ta_6C_5, TiC, V_2AlC
$(TiVZrNbMo)_2AlC$	Mo_3Al, $NbAl_3$, Nb_2AlC, Ti_3AlC_2, V_2AlC, ZrC	$(TiVZrNbHf)_2AlC$	HfC, Nb_2Al, Ti_3AlC_2, V_2Al, V_2AlC, $ZrAl_2$, Zr_6C_5
$(TiVZrNbTa)_2AlC$	Nb_2Al, Nb_2AlC, Ta_2C, Ti_3AlC_2, V_2AlC, $ZrAl_2$, Zr_6C_5	$(TiVZrMoTa)_2AlC$	Mo_3Al, Mo_3Al_8, Ta_2C, Ti_3AlC_2, V_2AlC, $ZrAl_2$, ZrC

$(TiVZrHfTa)_2AlC$	HfC, Ta_2C, Ti_3AlC_2, V_2AlC, V_2Ta, $ZrAl_2$, Zr_6C_5	$(TiVNbMoHf)_2AlC$	HfC, Mo_3Al, $NbAl_3$, Nb_2AlC, Ti_3AlC_2, V_2AlC
$(TiVNbMoTa)_2AlC$	Mo_3Al, $NbAl_3$, Nb_2AlC, Nb_6C_5, Ta_6C_5, Ti_6C_5, V_2AlC	$(TiVNbHfTa)_2AlC$	HfC, $NbAl_3$, Nb_2Al, Ta_2C, Ti_2AlC, V_2AlC
$(TiVMoHfTa)_2AlC$	HfC, Mo_3Al, Mo_3Al_8, Ta_2C, Ti_2AlC, V_2AlC	$(TiCrNbMoTa)_2AlC$	Cr_2Al, Mo_3Al, Mo_3Al_8, Nb_2AlC, Nb_6C_5, Ta_6C_5, TiC
$(TiZrNbMoHf)_2AlC$	HfC, Mo_3Al, $NbAl_3$, Nb_2AlC, Ti_3AlC_2, $ZrAl_2$, Zr_6C_5	$(TiZrNbMoTa)_2AlC$	Mo_3Al, $NbAl_3$, Nb_2AlC, Ta_2C, Ti_6C_5, ZrC
$(TiZrNbHfTa)_2AlC$	HfC, Nb_2Al, Nb_2AlC, Ta_2C, Ti_3AlC_2, $ZrAl_2$, Zr_6C_5	$(TiZrMoHfTa)_2AlC$	HfC, Mo_3Al, Mo_3Al_8, Ta_2C, Ti_3AlC_2, $ZrAl_2$, ZrC
$(TiNbMoHfTa)_2AlC$	HfC, Mo_3Al, $NbAl_3$, Nb_2AlC, Ta_2C, Ti_6C_5	$(VCrNbMoTa)_2AlC$	Cr_2Al, Mo_3Al, Mo_3Al_8, Nb_6C_5, Ta_6C_5, V_6C_5
$(VZrNbMoTa)_2AlC$	MoTa, Mo_3Al, $NbAl_3$, Nb_2AlC, Ta_6C_5, V_2AlC, ZrC	$(VZrNbHfTa)_2AlC$	HfC, Nb_2Al, Nb_2AlC, Ta_2C, V_2AlC, $ZrAl_2$, Zr_6C_5
$(VNbMoHfTa)_2AlC$	HfC, MoTa, Mo_3Al, $NbAl_3$, Nb_2AlC, Ta_6C_5, V_2AlC	$(ZrNbMoHfTa)_2AlC$	HfC, Mo_3Al, $NbAl_3$, Nb_2AlC, Ta_2C, $ZrAl_2$, ZrC
$(TiVCrNbMo)_3AlC_2$	Cr_3C_2, Mo_3Al, Mo_3Al_8, Nb_6C_5, TiC, V_6C_5	$(TiVCrNbTa)_3AlC_2$	C, $Cr_{23}C_6$, $NbAl_3$, Nb_6C_5, Ta_6C_5, TiC, V_6C_5
$(TiVCrMoTa)_3AlC_2$	Cr_7C_3, Mo_3Al, Mo_3Al_8, TaC, TiC, $Ti_2Mo_2C_3$, V_6C_5	$(TiVZrNbMo)_3AlC_2$	Mo_3Al, Mo_3Al_8, Nb_6C_5, TiC, V_2AlC, ZrC
$(TiVZrNbHf)_3AlC_2$	HfC, Nb_2Al, Nb_2AlC, Ti_3AlC_2, V_2AlC, $ZrAl_2$, Zr_6C_5	$(TiVZrNbTa)_3AlC_2$	$NbAl_3$, Nb_2AlC, Ta_2C, Ta_6C_5, Ti_3AlC_2, V_2AlC, ZrC
$(TiVZrMoTa)_3AlC_2$	Mo_3Al, Mo_3Al_8, Ta_6C_5, TiC, V_2AlC, ZrC	$(TiVZrHfTa)_3AlC_2$	HfC, Ta_2C, Ti_3AlC_2, V_2AlC, $ZrAl_2$, $ZrAl_3$, ZrC
$(TiVNbMoHf)_3AlC_2$	HfC, Mo_3Al, Mo_3Al_8, Nb_6C_5, TiC, V_2AlC	$(TiVNbMoTa)_3AlC_2$	Mo_3Al, Mo_3Al_8, Nb_2AlC, Nb_6C_5, Ta_6C_5, TiC, V_6C_5
$(TiVNbHfTa)_3AlC_2$	HfC, $NbAl_3$, Nb_3Al_2C, Nb_6C_5, Ta_2C, Ti_6C_5, V_2AlC	$(TiVMoHfTa)_3AlC_2$	HfC, Mo_3Al, Mo_3Al_8, Ta_6C_5, TiC, V_2AlC
$(TiCrNbMoTa)_3AlC_2$	Cr_7C_3, Mo_3Al, Mo_3Al_8, Nb_6C_5, TaC, TiC, $Ti_2Mo_2C_3$	$(TiZrNbMoHf)_3AlC_2$	HfC, Mo_3Al, Mo_3Al_8, Nb_2AlC, Ti_6C_5, ZrC
$(TiZrNbMoTa)_3AlC_2$	Mo_3Al, Mo_3Al_8, Nb_2AlC, Ta_6C_5, TiC, ZrC	$(TiZrNbHfTa)_3AlC_2$	HfC, $NbAl_3$, Nb_2AlC, Ta_2C, Ti_3AlC_2, Zr_6C_5
$(TiZrMoHfTa)_3AlC_2$	HfC, Mo_3Al, Mo_3Al_8, Ta_2C, Ta_6C_5, Ti_3AlC_2, ZrC	$(TiNbMoHfTa)_3AlC_2$	HfC, Mo_3Al, Mo_3Al_8, Nb_2AlC, Ta_6C_5, TiC
$(VZrNbMoTa)_3AlC_2$	Mo_3Al, Mo_3Al_8, Nb_6C_5, Ta_6C_5, V_2AlC, V_6C_5, ZrC	$(VZrNbHfTa)_3AlC_2$	HfC, $NbAl_3$, Nb_2AlC, Ta_2C, V_2AlC, ZrC, Zr_6C_5
$(ZrNbMoHfTa)_3AlC_2$	HfC, Mo_3Al, Mo_3Al_8, Nb_2AlC, Ta_6C_5, ZrC	$(TiVCrNbMo)_4AlC_3$	Cr_3C_2, MoC, Mo_3Al_8, Nb_6C_5, TiC, $Ti_2Mo_2C_3$, V_6C_5
$(TiVCrNbTa)_4AlC_3$	Cr_3C_2, Cr_7C_3, $NbAl_3$, Nb_6C_5, TaC, TiC, V_6C_5	$(TiVCrMoTa)_4AlC_3$	Cr_3C_2, Mo_3Al_8, TaC, TiC, $Ti_2Mo_2C_3$, VCr_3, V_6C_5
$(TiVZrNbMo)_4AlC_3$	$MoAl_3$, Mo_3Al, Nb_6C_5, TiC, $Ti_2Mo_2C_3$, V_6C_5, ZrC	$(TiVZrNbHf)_4AlC_3$	HfC, Nb_2AlC, TiC, Ti_3AlC_2, V_2AlC, ZrC
$(TiVZrNbTa)_4AlC_3$	$NbAl_3$, Nb_3AlC_2, Ta_6C_5, TiC, Ti_6C_5, V_2AlC, ZrC	$(TiVZrMoTa)_4AlC_3$	Mo_3Al, Mo_3Al_8, TaC, Ta_6C_5, TiC, V_6C_5, ZrC
$(TiVZrHfTa)_4AlC_3$	HfC, Ta_2C, Ta_3AlC_2, Ti_3AlC_2, V_2AlC, ZrC, Zr_2Al_3	$(TiVNbMoHf)_4AlC_3$	C, HfC, Mo_3Al, Mo_3Al_8, Nb_6C_5, TiC, V_6C_5
$(TiVNbMoTa)_4AlC_3$	Mo_3Al, Mo_3Al_8, Nb_6C_5, TaC, TiC, $Ti_2Mo_2C_3$, V_6C_5	$(TiVNbHfTa)_4AlC_3$	HfC, $NbAl_3$, Nb_3AlC_2, TaC, Ta_6C_5, Ti_6C_5, V_2AlC
$(TiVMoHfTa)_4AlC_3$	C, HfC, Mo_3Al, Mo_3Al_8, Ta_6C_5, TiC, V_6C_5	$(TiCrNbMoTa)_4AlC_3$	Cr_3C_2, Cr_7C_3, Mo_3Al_8, Nb_6C_5, TaC, TiC, $Ti_2Mo_2C_3$
$(TiZrNbMoHf)_4AlC_3$	HfC, Mo_3Al, Mo_3Al_8, $NbAl_3$, Nb_6C_5, TiC, ZrC	$(TiZrNbMoTa)_4AlC_3$	Mo_3Al, Mo_3Al_8, Nb_6C_5, TaC, Ta_6C_5, TiC, ZrC
$(TiZrNbHfTa)_4AlC_3$	HfC, $NbAl_3$, Nb_2AlC, TaC, Ta_2C, Ti_6C_5, ZrC	$(TiZrMoHfTa)_4AlC_3$	HfC, Mo_3Al, Mo_3Al_8, Ta_6C_5, TiC, Ti_6C_5, ZrC
$(TiNbMoHfTa)_4AlC_3$	HfC, Mo_3Al, Mo_3Al_8, Nb_6C_5, TaC, Ta_6C_5, TiC	$(VZrNbMoTa)_4AlC_3$	Mo_3Al_8, Nb_3Mo_{13}, Nb_6C_5, Ta_6C_5, V_6C_5, ZrC, $Zr_2Mo_2C_3$
$(VZrNbHfTa)_4AlC_3$	HfC, $NbAl_3$, Nb_2Al, Nb_2AlC, Ta_6C_5, V_2AlC, ZrC	$(ZrNbMoHfTa)_4AlC_3$	HfC, Mo_3Al, Mo_3Al_8, Nb_6C_5, TaC, Ta_6C_5, ZrC
$(TiVZrNbTa)_3SiC_2$	Nb_6C_5, TaC, TiC, V_6C_5, ZrSi, Nb_5Si_3C, $NbSi_2$	$(TiVZrHfTa)_3SiC_2$	HfC, Ta_6C_5, TiC, V_6C_5, V_5Si_3C, VSi_2, ZrSi
$(TiVNbHfTa)_3SiC_2$	HfC, Ta_6C_5, V_6C_5, Ti_3SiC_2, V_5Si_3C, Nb_5Si_3C, $NbSi_2$	$(TiZrNbHfTa)_3SiC_2$	C, HfC, TaC, TiC, SiC, ZrSi, Nb_5Si_3C
$(TiVZrNbHf)_4SiC_3$	HfC, Nb_6C_5, TiC, V_6C_5, SiC, V_5Si_3C, ZrSi	$(TiVZrNbTa)_4SiC_3$	Nb_6C_5, TaC, TiC, V_6C_5, ZrC, ZrSi, $NbSi_2$
$(TiVZrHfTa)_4SiC_3$	HfC, TaC, TiC, V_6C_5, VSi_2, $ZrSi_2$, ZrSi	$(TiVNbHfTa)_4SiC_3$	HfC, Ta_2C, Ta_6C_5, TiC, V_6C_5, Nb_5Si_3C, $NbSi_2$
$(TiZrNbMoTa)_4SiC_3$	C, Nb_6C_5, Ta_6C_5, TiC, ZrC, $MoSi_2$, Mo_5Si_3	$(TiZrNbHfTa)_4SiC_3$	HfC, Nb_6C_5, Ta_6C_5, TiC, SiC, Ti_3SiC_2, ZrSi
$(VZrNbHfTa)_4SiC_3$	HfC, Ta_2C, Ta_6C_5, V_6C_5, ZrC, Nb_5Si_3C, $NbSi_2$		

* $(TiVCrNb)_2AlC \longleftrightarrow \frac{1}{4}V_2AlC + \frac{1}{8}NbAl_3 + \frac{1}{8}Nb_3AlC_2 + \frac{1}{4}Cr_2Al + \frac{1}{2}TiC$. Each coefficients of the competing phases can be easily calculated by a linear equations.

Table S4 List of predicted HE-MXenes using chemical exfoliation energy. Synthesized HE-MXene compounds reported to date are highlighted in bold.

Type (Total number)	Predicted HE-MXenes
4-$M_{n+1}C_n$ (81)	$(TiVCrNb)_2C$, $(TiVCrMo)_2C$, $(TiVCrTa)_2C$, $(TiVZrNb)_2C$, $(TiVZrMo)_2C$, $(TiVZrHf)_2C$, $(TiVZrTa)_2C$, $(TiVNbMo)_2C$, $(TiVNbHf)_2C$, $(TiVNbTa)_2C$, $(TiVMoTa)_2C$, $(TiVHfTa)_2C$, $(TiCrNbMo)_2C$, $(TiCrNbTa)_2C$, $(TiCrMoTa)_2C$, $(TiZrNbMo)_2C$, $(TiZrNbHf)_2C$, **$(TiZrNbTa)_2C$**, $(TiZrMoTa)_2C$, $(TiZrHfTa)_2C$, $(TiNbMoHf)_2C$, $(TiNbMoTa)_2C$, $(TiNbHfTa)_2C$, $(TiMoHfTa)_2C$, $(VCrNbMo)_2C$, $(VZrNbMo)_2C$, $(VZrNbHf)_2C$, $(VZrNbTa)_2C$, $(VNbMoTa)_2C$, $(VNbHfTa)_2C$, $(ZrNbMoTa)_2C$, $(ZrNbHfTa)_2C$, $(TiVCrNb)_3C_2$, $(TiVCrMo)_3C_2$, $(TiVCrTa)_3C_2$, $(TiVZrNb)_3C_2$, $(TiVZrTa)_3C_2$, $(TiVNbMo)_3C_2$, $(TiVNbHf)_3C_2$, $(TiVNbTa)_3C_2$, $(TiVMoTa)_3C_2$, $(TiVHfTa)_3C_2$, $(TiZrNbMo)_3C_2$, $(TiZrNbHf)_3C_2$, $(TiZrNbTa)_3C_2$, $(TiZrMoTa)_3C_2$, $(TiZrHfTa)_3C_2$, $(TiNbMoHf)_3C_2$, $(TiNbMoTa)_3C_2$, $(TiNbHfTa)_3C_2$, $(TiMoHfTa)_3C_2$, $(VZrNbTa)_3C_2$, $(VNbHfTa)_3C_2$, $(ZrNbMoTa)_3C_2$, $(ZrNbHfTa)_3C_2$, **$(TiVCrMo)_4C_3$**, $(TiVCrTa)_4C_3$, $(TiVZrNb)_4C_3$, $(TiVZrTa)_4C_3$, **$(TiVNbMo)_4C_3$**, $(TiVNbTa)_4C_3$, $(TiVMoTa)_4C_3$, $(TiVHfTa)_4C_3$, $(TiCrNbTa)_4C_3$, $(TiZrNbMo)_4C_3$, $(TiZrNbHf)_4C_3$, $(TiZrNbTa)_4C_3$, $(TiZrMoTa)_4C_3$, $(TiZrHfTa)_4C_3$, $(TiNbMoHf)_4C_3$, $(TiNbMoTa)_4C_3$, $(TiNbHfTa)_4C_3$, $(TiMoHfTa)_4C_3$, $(VZrNbTa)_4C_3$, $(VNbMoTa)_4C_3$, $(VNbHfTa)_4C_3$, $(ZrNbMoHf)_4C_3$, $(ZrNbMoTa)_4C_3$, $(ZrNbHfTa)_4C_3$, $(ZrMoHfTa)_4C_3$, $(NbMoHfTa)_4C_3$
5-$M_{n+1}C_n$ (65)	$(TiVCrNbMo)_2C$, $(TiVCrNbTa)_2C$, $(TiVCrMoTa)_2C$, $(TiVZrNbMo)_2C$, $(TiVZrNbHf)_2C$, **$(TiVZrNbTa)_2C$**, $(TiVZrMoTa)_2C$, $(TiVZrHfTa)_2C$, $(TiVNbMoHf)_2C$, $(TiVNbMoTa)_2C$, $(TiVNbHfTa)_2C$, $(TiVMoHfTa)_2C$, $(TiCrNbMoTa)_2C$, $(TiZrNbMoHf)_2C$, $(TiZrNbMoTa)_2C$, $(TiZrNbHfTa)_2C$, $(TiZrMoHfTa)_2C$, $(TiNbMoHfTa)_2C$, $(VCrNbMoTa)_2C$, $(VZrNbMoTa)_2C$, $(VZrNbHfTa)_2C$, $(VNbMoHfTa)_2C$, $(ZrNbMoHfTa)_2C$, $(TiVCrNbMo)_3C_2$, $(TiVCrNbTa)_3C_2$, $(TiVCrMoTa)_3C_2$, $(TiVZrNbMo)_3C_2$, $(TiVZrNbHf)_3C_2$, $(TiVZrNbTa)_3C_2$, $(TiVZrMoTa)_3C_2$, $(TiVZrHfTa)_3C_2$, $(TiVNbMoHf)_3C_2$, $(TiVNbMoTa)_3C_2$, $(TiVNbHfTa)_3C_2$, $(TiVMoHfTa)_3C_2$, $(TiCrNbMoTa)_3C_2$, $(TiZrNbMoHf)_3C_2$, $(TiZrNbMoTa)_3C_2$, $(TiZrNbHfTa)_3C_2$, $(TiZrMoHfTa)_3C_2$, $(TiNbMoHfTa)_3C_2$, $(VZrNbMoTa)_3C_2$, $(VZrNbHfTa)_3C_2$, $(ZrNbMoHfTa)_3C_2$, $(TiVCrNbMo)_4C_3$, **$(TiVCrNbTa)_4C_3$**, $(TiVCrMoTa)_4C_3$, $(TiVZrNbMo)_4C_3$, $(TiVZrNbHf)_4C_3$, $(TiVZrNbTa)_4C_3$, $(TiVZrMoTa)_4C_3$, $(TiVZrHfTa)_4C_3$, $(TiVNbMoHf)_4C_3$, $(TiVNbMoTa)_4C_3$, $(TiVNbHfTa)_4C_3$, $(TiVMoHfTa)_4C_3$, $(TiCrNbMoTa)_4C_3$, $(TiZrNbMoHf)_4C_3$, $(TiZrNbMoTa)_4C_3$, $(TiZrNbHfTa)_4C_3$, $(TiZrMoHfTa)_4C_3$, $(TiNbMoHfTa)_4C_3$, $(VZrNbMoTa)_4C_3$, $(VZrNbHfTa)_4C_3$, $(ZrNbMoHfTa)_4C_3$

ESI Note 6. Scatter plots of correlation

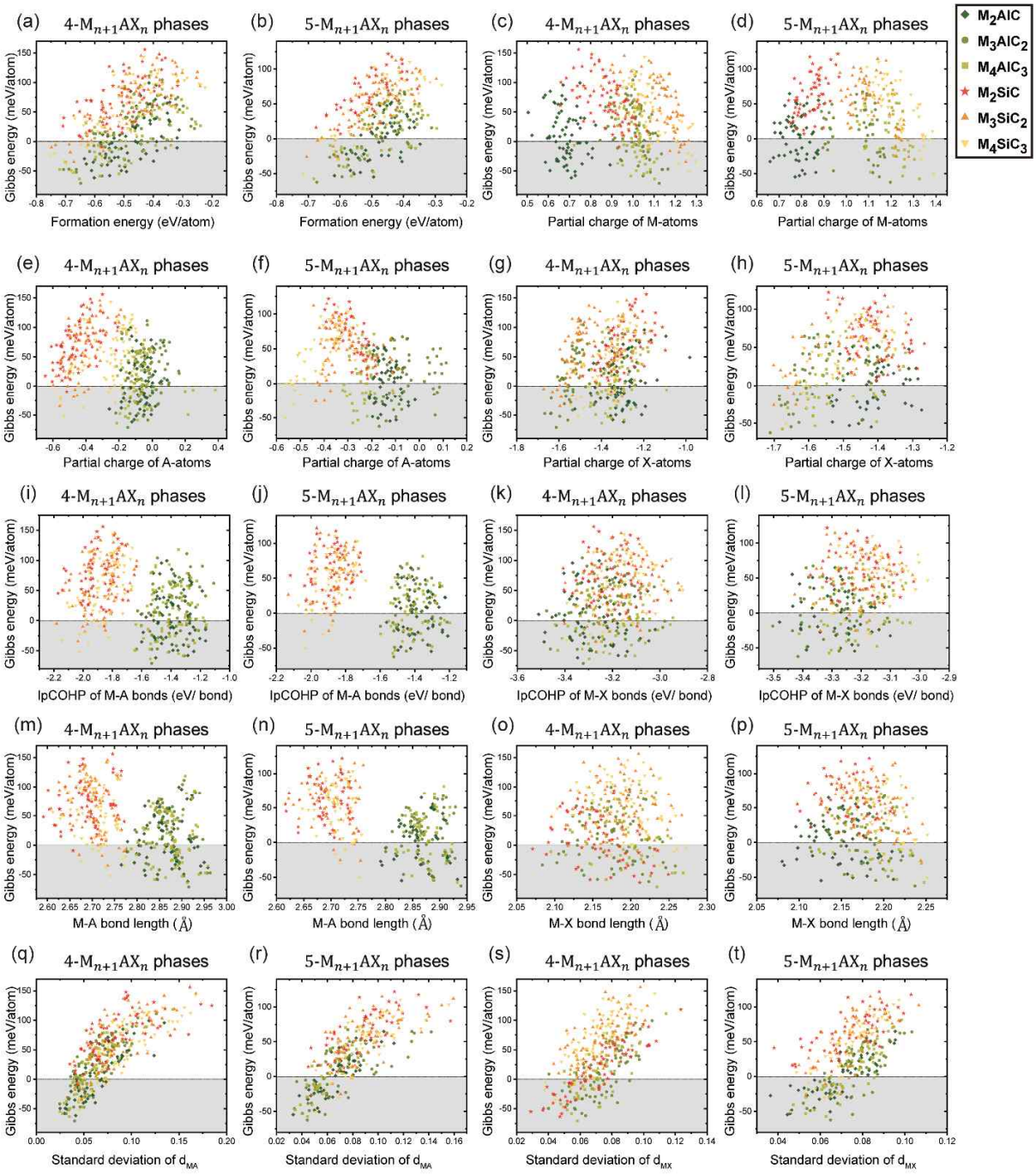

Fig. S3 For 4-$M_{n+1}AX_n$/5-$M_{n+1}AX_n$ phases, scatter plots show the correlation between the calculated relative Gibbs energy $\Delta G_{Re}^{1273\ K}$ and (a)/(b) formation energy, (c)/(d) partial charge of M-atoms, (e)/(f) partial charge of A-atoms, (g)/(h) partial charge of X-atoms, (i)/(j) M-A bond length, (k)/(l) M-X bond length, (m)/(n) standard deviation of M-A bond length, and (o)/(p) standard deviation of M-X bond length.

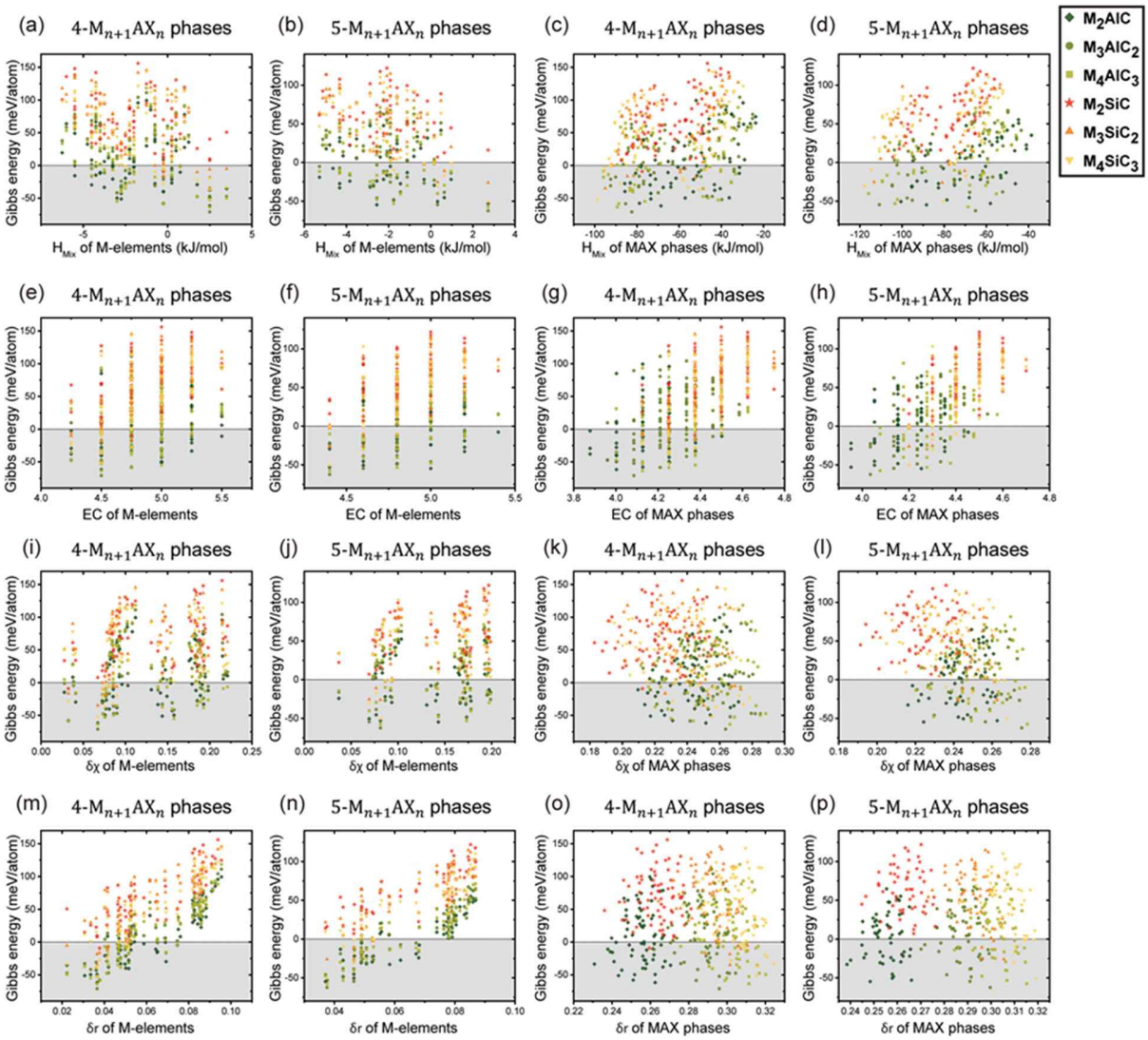

Fig. S4 For 4-$M_{n+1}AX_n$/5-$M_{n+1}AX_n$ phases, scatter plots show the correlation between the calculated relative Gibbs energy $\Delta G_{Re}^{1273\ K}$ and (a)/(b) mixing enthalpy of M-elements, (c)/(d) mixing enthalpy of HE-MAX phases, (e)/(f) average electron concentration of M-elements, (g)/(h) average electron concentration of HE-MAX phases, (i)/(j) differences in electronegativity of M-elements, (k)/(l) differences in electronegativity of HE-MAX phases, (m)/(n) differences in atomic radii of M-elements, and (o)/(p) differences in atomic radii of HE-MAX phases.

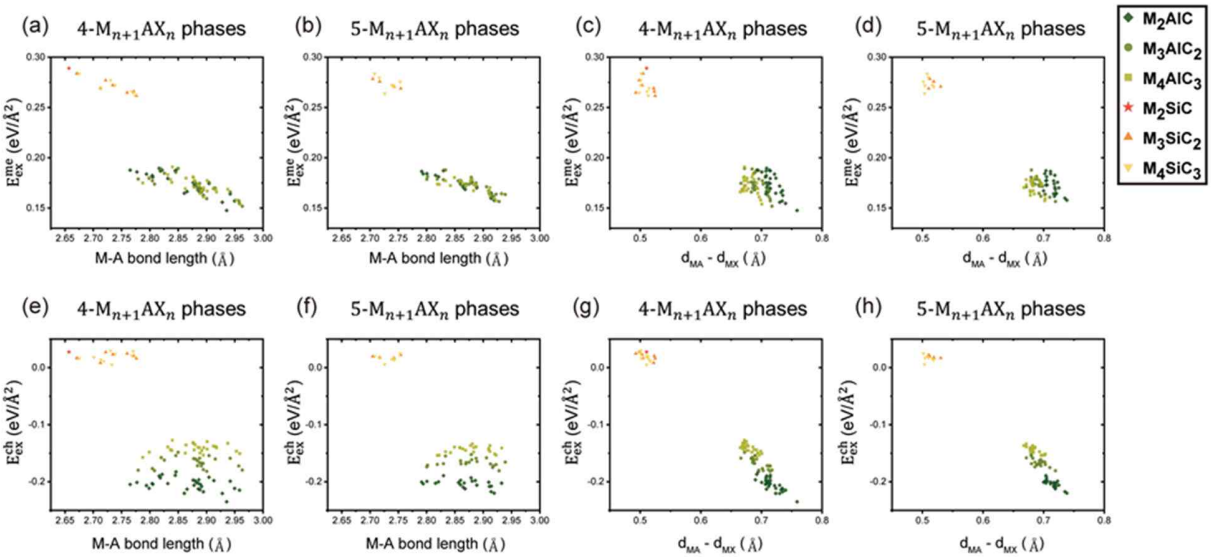

Fig. S5 For 4-$M_{n+1}AX_n$/5-$M_{n+1}AX_n$ phases, scatter plots show the correlation between (a)/(b) mechanical exfoliation energy and M-A bond length, (c)/(d) mechanical exfoliation energy and differences in M-A bond length and M-X bond length, (e)/(f) chemical exfoliation energy and M-A bond length, and (g)/(h) chemical exfoliation energy and differences in M-A bond length and M-X bond length.

ESI Note 7. 3D plot of the charge density difference

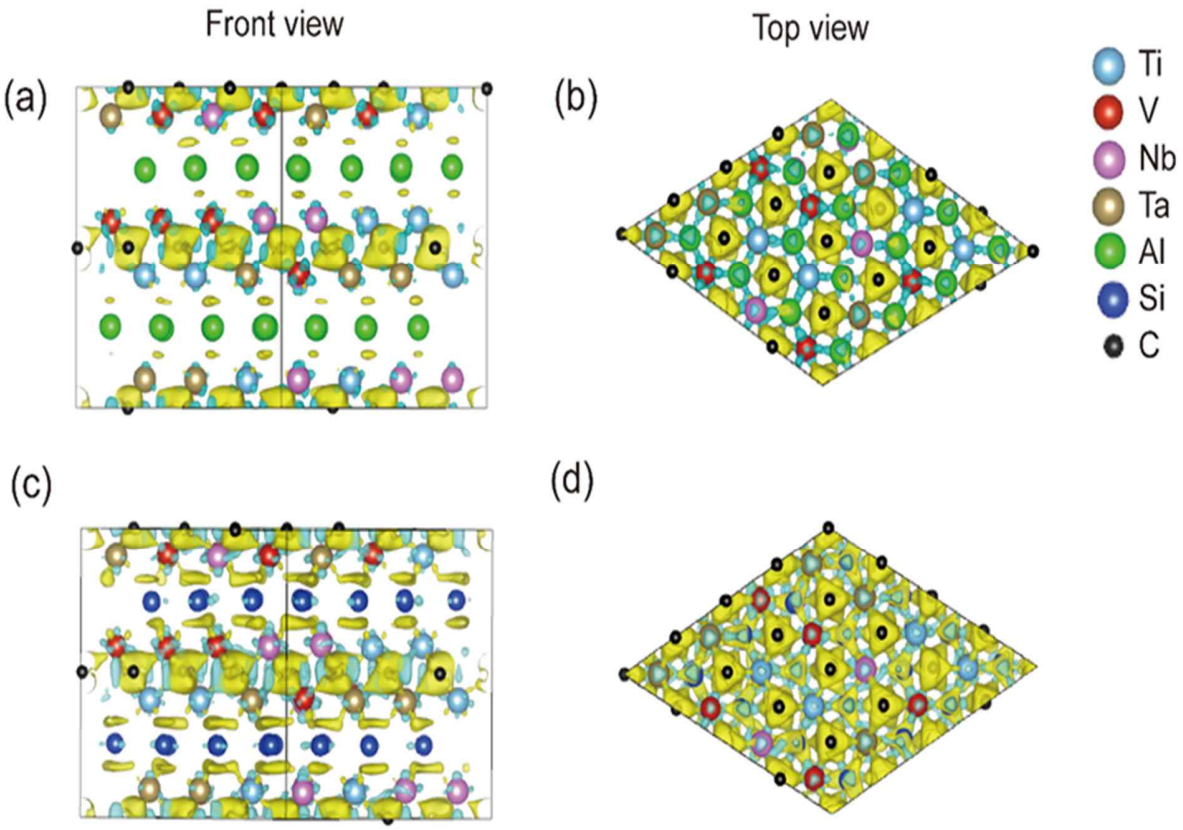

Fig. S6 3D data display of the (a), (b) charge density difference in $(TiVNbTa)_2AlC$ structure and (c),(d) charge density difference in $(TiVNbTa)_2SiC$ structure. The charge density difference (Δρ) was calculated as ρ(MAX) – ρ(M-layers) – ρ(A-layers) – ρ(X-layers).

ESI Note 8. TDOS and pCOHP

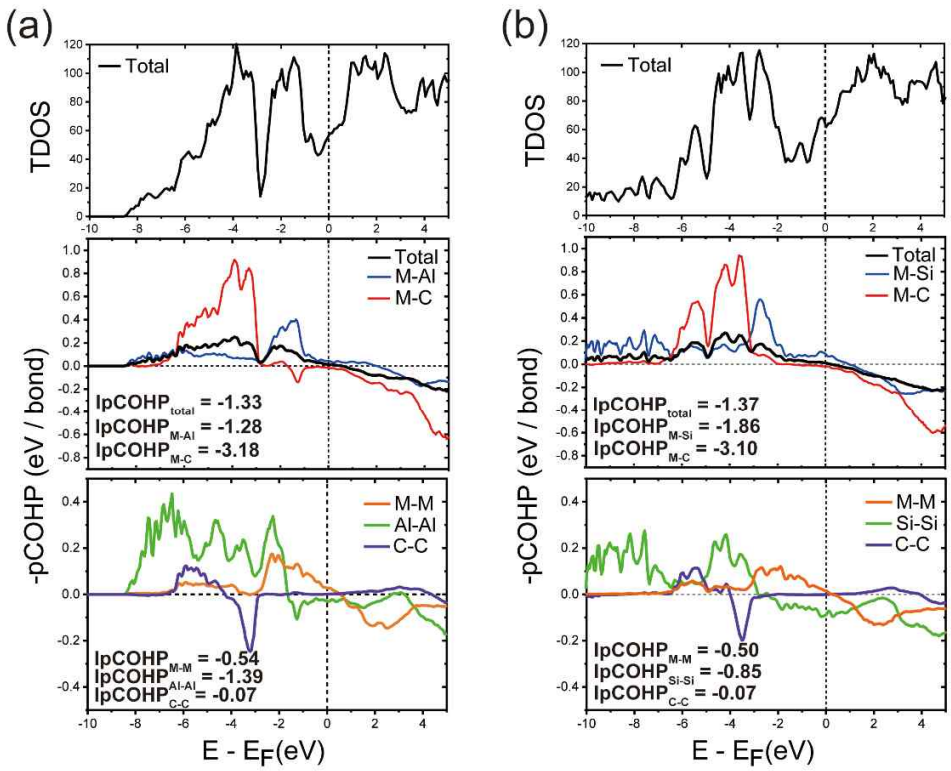

Fig. S7 Plots of total density of states (TDOS) and -pCOHP of (a) $(TiVNbTa)_2AlC$ and (b) $(TiVNbTa)_2SiC$

ESI Note 9. Average values of the mechanical exfoliation energy, chemical exfoliation energy, and lattice parameter

Table S5 Average values of the mechanical exfoliation energy ($\overline{E_{ex}^{m\,e}}$), chemical exfoliation energy ($\overline{E_{ex}^{ch}}$), and lattice parameter ($\bar{a}$) according to the number of layers of the HE-$M_{n+1}AX_n$ phases. And Average values of the mechanical exfoliation energy ($\overline{E_{ex}^{m\,e}}$) of the single M-MAX phases.[18]

	$\overline{\mathbf{E}_{\mathbf{ex}}^{\boldsymbol{m}\,\boldsymbol{e}}}$ (eV/Å^2)	$\overline{\mathbf{E}_{\mathbf{ex}}^{\boldsymbol{ch}}}$ (eV/atom)	$\overline{\boldsymbol{a}}$ (Å)	$\overline{\mathbf{E}_{\mathbf{ex}}^{\boldsymbol{m}\,\boldsymbol{e}}}$ (eV/unitcell)	$\overline{\mathbf{E}_{\mathbf{ex}}^{\boldsymbol{m}\,\boldsymbol{e}}}$ (eV/Å^2) (Ref[18])
M_2AlC	0.173	-0.204	3.082	5.706	0.182
M_3AlC_2	0.172	-0.167	3.107	5.786	0.175
M_4AlC_3	0.172	-0.143	3.109	5.798	0170
M_2SiC	0.289	0.027	3.124	9.593	0.184
M_3SiC_2	0.272	0.019	3.126	9.476	0.174
M_4SiC_3	0.275	0.018	3.123	9.474	0.168

REFERENCES

1 V. J. Keast, S. Harris and D. K. Smith, *Phys. Rev. B - Condens. Matter Mater. Phys.*, 2009, **80**, 1–7.

2 M. Dahlqvist, B. Alling and J. Rosén, *Phys. Rev. B - Condens. Matter Mater. Phys.*, 2010, **81**, 1–4.

3 A. Thore, M. Dahlqvist, B. Alling and J. Rosén, *Comput. Mater. Sci.*, 2014, **91**, 251–257.

4 O. F. Dippo and K. S. Vecchio, *Scr. Mater.*, 2021, **201**, 113974.

5 M. Dahlqvist and J. Rosen, *Phys. Chem. Chem. Phys.*, 2015, **17**, 31810–31821.

6 M. N. Gjerding, A. Taghizadeh, A. Rasmussen, S. Ali, F. Bertoldo, T. Deilmann, N. R. Knøsgaard, M. Kruse, A. H. Larsen, S. Manti, T. G. Pedersen, U. Petralanda, T. Skovhus, M. K. Svendsen, J. J. Mortensen, T. Olsen and K. S. Thygesen, *2D Mater.*, 2021, **8**, 044002, DOI:10.1088/2053-1583/ac1059.

7 I. Opahle, G. K. H. Madsen and R. Drautz, *Phys. Chem. Chem. Phys.*, 2012, **14**, 16197–16202.

8 V. Stevanović, S. Lany, X. Zhang and A. Zunger, *Phys. Rev. B - Condens. Matter Mater. Phys.*, 2012, **85**, 1–12.

9 A. Benisek and E. Dachs, *Contrib. to Mineral. Petrol.*, 2018, **173**, 1–11.

10 J. E. Saal, S. Kirklin, M. Aykol, B. Meredig and C. Wolverton, *Jom*, 2013, **65**, 1501–1509.

11 S. Kirklin, J. E. Saal, B. Meredig, A. Thompson, J. W. Doak, M. Aykol, S. Rühl and C. Wolverton, *npj Comput. Mater.*, 2015, **1**, 15010, DOI:10.1038/npjcompumats.2015.10.

12 D. B. Miracle and O. N. Senkov, *Acta Mater.*, 2017, **122**, 448–511.

13 M. Naguib, M. Kurtoglu, V. Presser, J. Lu, J. Niu, M. Heon, L. Hultman, Y. Gogotsi and M. W. Barsoum, *Adv. Mater.*, 2011, **23**, 4248–4253.

14 M. Khazaei, M. Arai, T. Sasaki, M. Estili and Y. Sakka, *Sci. Technol. Adv. Mater.*, 2014, **15**, 014208, DOI:10.1088/1468-6996/15/1/014208.

15 M. Khazaei, A. Ranjbar, K. Esfarjani, D. Bogdanovski, R. Dronskowski and S. Yunoki, *Phys. Chem. Chem. Phys.*, 2018, **20**, 8579–8592.

16 E. M. D. Siriwardane, R. P. Joshi, N. Kumar and D. Çaklr, *ACS Appl. Mater. Interfaces*, 2020, **12**, 29424–29431.

17 D. Dolz, Á. Morales-García, F. Viñes and F. Illas, *Nanomaterials*, 2021, **11**, 1–12.

18 R. Khaledialidusti, M. Khazaei, S. Khazaei and K. Ohno, *Nanoscale*, 2021, **13**, 7294–7307.

19 S. Zhao, G. M. Stocks and Y. Zhang, *Acta Mater.*, 2017, **134**, 334–345.

20 J. D. Strother and C. Z. Hargather, *Materialia*, 2020, **14**, 100927, DOI:10.1016/j.mtla.2020.100927.

21 N. C. Frey, J. Wang, G. I. Vega Bellido, B. Anasori, Y. Gogotsi and V. B. Shenoy, *ACS Nano*, 2019, **13**, 3031–3041.